Received: 13 October 2023 | Revised: 2 February 2024 | Accepted: 9 February 2024

DOI: 10.1111/gcb.17231

Global Change Biology WILEY

RESEARCH ARTICLE

Decoding autumn phenology: Unraveling the link between observation methods and detected environmental cues

Simon Kloos[1] | Anne Klosterhalfen[2] | Alexander Knohl[2,3] | Annette Menzel[1,4]

[1]TUM School of Life Sciences, Ecoclimatology, Technical University of Munich, Freising, Germany

[2]Bioclimatology, University of Göttingen, Göttingen, Germany

[3]Centre of Biodiversity and Sustainable Land Use (CBL), University of Göttingen, Göttingen, Germany

[4]Institute for Advanced Study, Technical University of Munich, Garching, Germany

Correspondence
Simon Kloos, TUM School of Life Sciences, Ecoclimatology, Technical University of Munich, Freising 85354, Germany.
Email: simon.kloos@tum.de

Funding information
Bavarian State Ministry of Science and the Arts; German Federal Ministry of Education and Research; Deutsche Forschungsgemeinschaft, Grant/Award Number: INST 186/1118-1 FUGG; Ministry of Lower-Saxony for Science and Culture, Grant/Award Number: ZN 3679

Abstract

Leaf coloring and fall mark the end of the growing season (EOS), playing essential roles in nutrient cycling, resource allocation, ecological interactions, and as climate change indicators. However, understanding future changes in autumn phenology is challenging due to the multitude of likely environmental cues and substantial variations in timing caused by different derivation methods. Yet, it remains unclear whether these two factors are independent or if methodological uncertainties influence the environmental cues determined. We derived start of growing season (SOS) and EOS at a mixed beech forest in Central Germany for the period 2000–2020 based on four different derivation methods using a unique long-term data set of in-situ data, canopy imagery, eddy covariance measurements, and satellite remote sensing data and determined their influence on a predictor analysis of leaf senescence. Both SOS and EOS exhibited substantial ranges in mean onset dates (39.5 and 28.6 days, respectively) across the different methods, although inter-annual variations and advancing SOS trends were similar across methods. Depending on the data, EOS trends were advanced or delayed, but inter-annual patterns correlated well (mean $r = .46$). Overall, warm, dry, and less photosynthetically productive growing seasons were more likely to be associated with a delayed EOS, while colder, wetter, and more photosynthetically productive vegetation periods resulted in an earlier EOS. In addition, contrary to recent results, no clear influence of pre-solstice vegetation activity on the timing of senescence was detected. However, most notable were the large differences in sign and strength of potential drivers both in the univariate and multivariate analyses when comparing derivation methodologies. The results suggest that an ensemble analysis of all available phenological data sources and derivation methods is needed for general statements on autumn phenology and its influencing variables and correct implementation of the senescence process in ecosystem models.

KEYWORDS
eddy covariance, end of season, Hainich, ICOS, leaf coloring, phenocam, photosynthesis, remote sensing, temperature, water availability

1 | INTRODUCTION

Autumn phenology significantly determines biogeochemical cycles in terrestrial ecosystems, such as the carbon cycle (Keenan et al., 2014; Piao et al., 2007; Richardson et al., 2010; Wu, Chen, et al., 2013; Wu, Gough, et al., 2013) or the water cycle (Gaertner et al., 2019; Kim et al., 2018), by directly ending carbon uptake or evapotranspiration. These changes in the growing season also exert biophysical feedback on the climate system (Peñuelas et al., 2009; Richardson et al., 2013; Stéfanon et al., 2012). In the past, a general trend towards a delay in autumn senescence has been observed in the northern hemisphere, whereby the magnitude, direction, and significance of the autumn phenological trends differ significantly depending on the species, the observation period, and the study region (Garonna et al., 2016; Gill et al., 2015; Liu, Fu, Zhu, et al., 2016; Menzel & Fabian, 1999; Menzel et al., 2020; Piao et al., 2019). To explain these observed features as well as to model and forecast future autumn phenology, it is of tremendous importance to fully understand all (environmental) drivers of leaf senescence; however, recent studies found varying and contradicting results.

The temperature is a main driver for leaf discoloration and leaf fall of deciduous trees in autumn (Gallinat et al., 2015; Gill et al., 2015), however with varying seasonal and daily patterns. Numerous current studies have shown that higher temperatures before senescence or all-year warming result in a delay in the phenological autumn (Fu et al., 2018; Lang et al., 2019; Liu, Fu, Zeng, et al., 2016; Liu, Fu, Zhu, et al., 2016; Menzel et al., 2020; Zohner & Renner, 2019). However, mostly likely due to different temporal resolutions and influencing periods, several studies have shown a differentiated picture in this temperature-senescence relationship: Chen et al. (2020) noted a delay in leaf coloration only with warming night-time temperatures—while warmer daytime temperatures cause it to start earlier. Estrella and Menzel (2006), Liu et al. (2018), and Lu and Keenan (2022) detected a delay in autumn phenology only with warmer autumn temperatures but not with higher temperatures in summer or in the growing season. This could be because heat stress was shown to lead to earlier rather than later autumn phenology (Xie et al., 2015, 2018). Furthermore, Zohner et al. (2023) recently noted a solstice effect in temperature, with increased temperatures before solstice leading to earlier senescence and after solstice leading to a lengthening of the autumn growing season. Finally, temperature-related effects on senescence seem to be also species-dependent (Grossiord et al., 2022).

Besides air temperature, other factors have also been studied to trigger leaf coloring and leaf fall in autumn. Water availability, characterized by precipitation amounts, soil moisture or vapor pressure deficit, has been frequently tested, but the results are also contradictory. While drier conditions are generally associated with earlier senescence (Gill et al., 2015), there are also study results that ascribe no or even opposite effects of water availability on autumn phenology (Estrella & Menzel, 2006; Liu et al., 2018; Xie et al., 2015, 2018; Zani et al., 2020). The study region, the biome, the type of phenology recorded, and the tree species also represent differentiating factors in this relationship (Bigler & Vitasse, 2021; Grossiord et al., 2022; Liu, Fu, Zeng, et al., 2016; Liu, Fu, Zhu, et al., 2016; Lu & Keenan, 2022). Other less considered and discussed factors for autumn senescence are photoperiod (Gill et al., 2015; Lang et al., 2019), nutrient availability (Fu et al., 2019), insolation (Liu, Fu, Zeng, et al., 2016; Liu, Fu, Zhu, et al., 2016; Lu & Keenan, 2022), and legacy or carryover effects, such as the timing of preceding leaf unfolding (Fu et al., 2019; Keenan & Richardson, 2015; Liu, Fu, Zhu, et al., 2016; Zani et al., 2020), and—more recently—growing season photosynthesis (Lu & Keenan, 2022; Norby, 2021; Zani et al., 2020; Zohner et al., 2023).

In addition to the multiple potential factors influencing autumn phenology, there is also a second source of uncertainty for future predictions: the used datasets and methods to derive phenological events. While many studies have compared remote sensing and ground-observed phenology (e.g., Berra & Gaulton, 2021; Mariën et al., 2019), only a few studies—mostly based in the US—have compared multiple data sources in autumn phenology. For mixed forests, Garrity et al. (2011) observed little agreement, while Zhao et al. (2020) found just minor differences between remote sensing derived and ground-observed autumn phenology. In contrast, Melaas et al. (2016) found varying correlations between autumn phenology from satellite remote sensing, eddy covariance measurements, canopy images and in-situ observations in North America, depending on the study area and data source. The spatial resolution of the data and the tree species composition may play a major role in this context (Klosterman et al., 2018). Accordingly, for deciduous forests in Europe, significant differences in the autumn phenology from remote sensing indices, eddy covariance measurements, and ground-based observations, such as in-situ or camera data, have been reported (Jin et al., 2017; Soudani et al., 2021). In contrast, comparatively good agreement was obtained by Liu et al. (2019) for leaf fall in a Chinese deciduous forest, using radiometer as well as satellite remote sensing data and leaf-litterfall measurements. Thus, D'Odorico et al. (2015) concluded on the phenological data mismatch for the entire northern hemisphere, that depending on the data source, derivation methodology, period and study site, the autumn phenology of deciduous forests is only partially (if at all) consistent with other data sources.

Based on the research findings regarding autumn phenology in deciduous forests, two imminent research gaps merge: First, there are hardly any detailed and long-term evaluations in Central Europe comparing different data sources for deriving autumn phenology. Second, most studies investigating the tricky influential factors of autumn phenology of deciduous forests rely on a single data source for phenology derivation, despite the potentially significant differences in derived phenology among datasets. To our knowledge, no study has explored the combined impact of these two sources of uncertainty. Consequently, there is a knowledge gap on how divergent phenological metrics further complicate the identification of drivers of autumn phenology. This study addresses these gaps through a detailed analysis of long-term data from Hainich National Park, Germany, which has one of the longest time series of canopy camera (CC) datasets in combination with continuous eddy covariance

measurements worldwide. Our research aims to answer the following key research questions:

1. What are the differences in spring and autumn phenology of a European deciduous forest when derived indirectly from satellite remote sensing data and eddy covariance measurements or directly from canopy imagery and in-situ phenological observations?
2. How do uncertainties and variations in derived phenology impact the univariate and multivariate analysis of potential factors influencing early, mid, and late autumn phenology in deciduous forests?

2 | MATERIALS AND METHODS

2.1 | Study site

The study site with its associated flux tower is located in Central Europe in the Hainich National Park (51.079407°N, 10.452089°E; 440 m a.s.l.; Germany; Figure 1). The National Park with an area of approximately 7600 ha was established for beech forest protection in 1997. Due to relatively undisturbed development, some trees are up to 270 years old. It has also been a UNESCO World Heritage Site since 2011 (Thiel et al., 2020). The forest of the National Park consists mainly of European beech (*Fagus sylvatica* L., 64%) and European ash (*Fraxinus excelsior* L., 28%; Tamrakar et al., 2018). During the study period from 2000 to 2020, the mean annual temperature at the flux tower site was 8.6°C, and the mean annual precipitation sum was 716 mm. The flux tower is located on a slightly inclined north slope (2°–3°; Knohl et al., 2003). Further information on the study area and location can be found in Knohl et al. (2003) or Tamrakar et al. (2018).

2.2 | In-situ phenology

Phenological observations are available from the network of the German Meteorological Service (DWD). The data set contains annual point measurements of 50 different phenological phases, which are then interpolated for a grid with a spatial resolution of 1 × 1 km over Germany: For this interpolation, Germany is

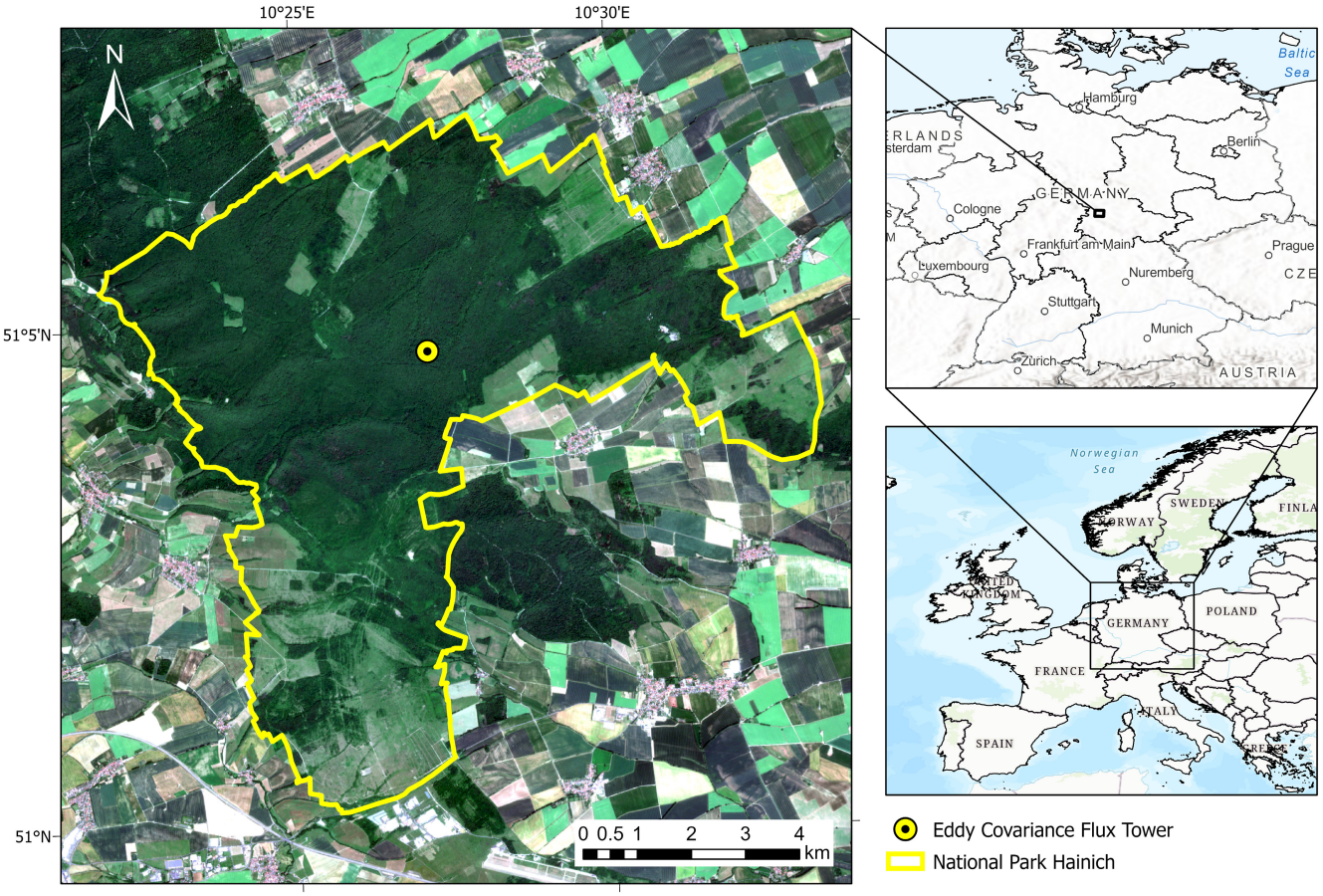

FIGURE 1 General map of Hainich National Park (left) and its location in Germany and Europe (right). The boundaries of the National Park are marked in yellow; the site of the eddy covariance flux tower is marked with a black and yellow dot (Source: Sentinel-2 [Copernicus SciHub], Esri, FAO, NOAA, USGS; GDI-Th, Earthstar Geographics; HERE, Garmin). Map lines delineate study areas and do not necessarily depict accepted national boundaries.

segmented into 20 regions, each comprising overlapping circles of uniform size. Within each region, all observations undergo multiple linear regression analysis, considering altitude, longitude, and latitude as regression coefficients. The regression coefficients for the four neighboring circles at a specific location are then weighted based on the distances to the circle centers. Finally, for each 1 × 1 km grid cell, annual onset dates are then interpolated based on these local regression coefficients (DWD Climate Data Center, 2022; Yuan et al., 2021).

The grid was used for the complete study period from 2000 to 2020. As the Hainich National Park mainly consists of beech forest, the dataset RBUBO (European beech—beginning of unfolding of leaves: the first leaves have entirely pushed out of the bud and unfolded up to the stalk; DWD:LU) was used for spring phenology, and the datasets RBUBV (European beech—autumn leaf coloring: about half of the leaves on the observation tree have turned autumnal; DWD:LC) and RBUBF (European beech—autumn leaf fall: about half the leaves of the observation tree have fallen off; DWD:LF) for autumn phenology. Unfortunately, leaf unfolding, coloring and fall of European ash are not part of the DWD phenological program, thus this phase could not be included in the in-situ data. Further information regarding the data can be found at DWD Climate Data Center (2022). The respective onset dates (DOY, day of year) were extracted bilinearly from all raster files for the coordinates of the flux tower.

2.3 | Satellite phenology

The remote sensing based phenology was extracted from the MODIS Land Cover Dynamics Product MCD12Q2 (Gray et al., 2019), which has been used in many studies dealing with remote sensing of phenology (e.g., Lu & Keenan, 2022; Zohner et al., 2023). Plant phenology is derived globally from 2-band Enhanced Vegetation Index (EVI) data with a resolution of 500 m. For spring phenology, the phases Greenup (date when EVI2 first crossed 15% of the segment EVI2 amplitude; MODIS:GU) and MidGreenup (date when EVI2 first crossed 50% of the segment EVI2 amplitude; MODIS:MGU) were used. For autumn phenology, the phases senescence (date when EVI2 last crossed 90% of the segment EVI2 amplitude; MODIS:SE) and dormancy (date when EVI2 last crossed 15% of the segment EVI2 amplitude; MODIS:DO) were used. Data were available from 2001 to 2019. To improve the quality of the data set, the quality assurance layer was applied to the existing raster files. The layer consists of scores (0 = "best"; 1 = "good"; 2 = "fair"; 3 = "poor"), which are composed of various criteria for calculating the phenology (fraction of missing or filled EVI data in the cycle, spline goodness-of-fit) for each pixel. In our study, we only used the highest quality class (=0) in the data set. Subsequently, the corresponding DOY for the respective phenological phase was extracted bilinearly from all raster files using the flux tower coordinates.

2.4 | CC phenology

The CC is placed on top of the flux tower above the tree canopy and provided recordings from 2001 to 2020. From 2001 to 2019, the pictures were always taken at 12:00 noon, since August 2020, every 30 min throughout the day. As the camera position changed a few times, and in some cases, there were longer data gaps in the dataset, the annual phenology could only be estimated visually from the pictures.

As far as the data availability for a year allowed, both start of season (SOS; BBCH 11 = first leaves unfold) and end of season (EOS; BBCH 95 = 50% of the leaves have fallen/discolored) were determined (for the BBCH (Biologische Bundesanstalt für Land- und Forstwirtschaft, Bundessortenamt und CHemische Industrie) coding see Meier, 2018). Due to the different camera positions, an individual region of interest (ROI) was created for each year and phase (SOS/EOS). The ROI was always set for the two main tree species of the Hainich National Park: *F. sylvatica* (CC:Fagus) and *F. excelsior* (CC:Fraxinus). The process of manually estimating the spring and autumn phenology via the CC images was carried out independently by three experienced and trained bioclimatologists. The mean of the three SOS/EOS estimates represented the respective CC phenology (CC:Fraxinus and CC:Fagus).

2.5 | Flux tower data

The data from the flux tower in the Hainich National Park are part of the Integrated Carbon Observation System (ICOS) network (DE-Hai; https://www.icos-cp.eu/) and cover the period 2000–2020 on a half-hourly or daily basis (Knohl et al., 2022). A variety of both meteorological and ecosystem CO_2 exchange-related variables are measured, but only the following variables were used in this study:

- Air temperature (°C)
- Precipitation (mm).
- Vapor pressure deficit (VPD) (hPa)
- Soil water content (16 cm depth) (%)
- Net ecosystem exchange (NEE) (g C m^{-2} day^{-1})
- Gross primary production, from daytime partitioning method (GPP:DT) (g C m^{-2} day^{-1})
- Gross primary production, from nighttime partitioning method (GPP:NT) (g C m^{-2} day^{-1})

Here, we included GPP derived from nighttime and from daytime flux-based partitioning methods, respectively, because they slightly differ in their approaches and assumptions (Wutzler et al., 2018). The nighttime source partitioning method (after Reichstein et al., 2005) first derives a relationship between (air or soil) temperature and the measured NEE during nighttime, which then only consists of respiratory fluxes. By extrapolating this temperature-respiration response function, ecosystem respiration (Reco) can also be estimated for daytime hours and with

calculating the balance between measured NEE and estimated Reco also GPP can be obtained. The daytime source partitioning method (after Lasslop et al., 2010) derives GPP and Reco during daytime based on a rectangular hyperbolic light-response curve, fitting this function to measured NEE data during daytime. Thus, this daytime source partitioning approach also considers the impact of varying meteorological conditions, such as incoming radiation and VPD, on GPP. Finally, Reco during nighttime is again derived based on a temperature-respiration response function.

2.5.1 | Flux tower phenology

To derive the phenology of Hainich National Park from the flux tower data, NEE, as well as GPP:DT and GPP:NT, were analyzed. Daily resolved data from 2000 to 2020 was used for all three variables. As a first step, all NEE values were converted to net ecosystem production (NEP) values (NEP = −NEE) to create a consistent positive sign for CO_2 uptake with NEP and GPP. To derive SOS and EOS from the NEP data, the smoothed-threshold approach was chosen (Barnard et al., 2018). A moving-window mean was calculated (central, 5 days) and a threshold of 0 g C m^{-2} day^{-1} was set. SOS was defined as the day this threshold value was overshot for the first time (CO_2 uptake) and remained overshot for 20 consecutive days. Inversely, EOS was defined as the day on which the NEP undershot the threshold value again for the first time and was no longer above it for 20 days in a row. The phenology of GPP:DT and GPP:NT was determined in a comparable method, but here the threshold was defined as a 10% value of the mean annual GPP maximum from 2000 to 2020 (Zhou et al., 2016, 2017). Thus, SOS was defined as the day this threshold value was exceeded for the first time in a year and EOS as the day this threshold was not met for the first time. In addition, SOS < 30 and EOS > 330 were discarded as extreme outliers.

2.5.2 | EOS predictor variables

To detect potential influencing factors on autumn phenology in Hainich National Park, 20 predictor variables from phenology, meteorology and ecosystem CO_2 exchange were selected and derived (Table 1) from literature including Zani et al. (2020). We additionally calculated a Dryness-Wetness Index (DWI) to incorporate the aspect of drought as a potential driver of autumn phenology. Since dryness/drought can be defined from different perspectives (Wilhite & Glantz, 1985), an index calculation combining different drought-related variables was chosen. For the annual DWI used in this study, six different variables were included in the index calculation:

- Growing season precipitation: Precipitation sum from March to October (mm)
- Summer precipitation: Precipitation sum in June, July, and August (mm)
- Growing season VPD: VPD sum from March to October (hPa)
- Summer VPD: VPD sum in June, July, and August (hPa)
- Growing season soil water content: Mean soil water content (16 cm depth) from March to October (%)
- Summer soil water content: Mean soil water content (16 cm depth) in June, July, and August (%)

For precipitation and for soil water content both in the growing season and in summer, the following index was calculated annually for the study period 2000–2020 on the basis of daily data:

$$\text{Index} = \frac{x_i - x_{\min}}{x_{\max} - x_{\min}}. \quad (1)$$

x_i represents the respective value of the year, x_{max} and x_{min}, the respective maxima and minima in the period from 2000 to 2020. The value range of the index is accordingly between 0 and 1. The closer the index is to 0, the drier the conditions in the respective year. An index was also calculated for the VPD both in the growing season and in summer:

$$\text{Index} = \frac{x_{\max} - x_i}{x_{\max} - x_{\min}}. \quad (2)$$

The variables are congruent with Equation (1); here, values range from 0 to 1. The closer the index is to 0, the drier the VPD conditions. Finally, all six calculated indices were added up annually and defined as DWI. The range of values here extends from 0 (*very dry*) to 6 (*very wet*).

2.6 | Statistical analyses

Phenological data were analyzed using descriptive statistics, including trend analysis via linear regression with the year as predictor over the observation period, as well as a Pearson-correlation analysis for the spring and autumn datasets. We identified the factors that influence autumn phenology using univariate and multivariate analyses. In the univariate analysis, we calculated Spearman-rank correlation coefficients between all EOS data and the predictor variables (see Section 2.5.2). For the multivariate analysis, a common predictor dataset from the three main predictor groups temperature, water availability and photosynthetic activity was selected from the 20 predictor variables. To achieve this, the previously calculated SOS variables from different data sources were averaged for each year. Subsequently, to prevent multicollinearity within the dataset, variables with a strong ($r > .7$) and statistically significant ($p < .05$) Spearman correlation coefficient (Table S1) were not included in the analysis. Finally, for all EOS data sets, multiple linear regressions with two and three predictor variable combinations were calculated and the individual models were compared with each other. For reasons of clarity, we have decided to show only the 3- and 2-predictor combinations of the most common temperature (T_{AU} and T_{SU}) and water availability (P_{HY}) variables as well as the only directly measured photosynthesis variable (NEP). Combinations with other variables from

TABLE 1 Predictor variables for autumn phenology used including abbreviation, description, and unit. The hydrological year runs from 01.11. of the previous year to 31.10. of the current year.

Variable	Abbreviation	Description	Unit
Start of season	SOS	Respective SOS of the data source, for MODIS: Greenup	Day of year
Summer temperature	T_{SU}	Mean daily temperature in June, July, and August	°C
Autumn temperature	T_{AU}	Mean daily minimum temperature in September and October	°C
Extreme heat events	T_{EX}	Number of days with maximum temperature >30°C in the hydrological year	Days
Frost days	F_{HY}	Number of days with minimum temperature <0°C in the hydrological year	Days
Frost days in spring	F_{SP}	Number of days with minimum temperature <0°C from SOS until 60 days later	Days
Annual precipitation	P_{HY}	Number of days with >2 mm precipitation in the hydrological year	Days
Summer precipitation	P_{SU}	Number of days with >2 mm precipitation in June, July, and August	Days
Heavy rain days	P_{EX}	Number of days with >20 mm precipitation in the hydrological year	Days
Growing season vapor pressure deficit	VPD	Sum of daily VPD between SOS and September (30 September/DOY: 274)	hPa
Dryness-Wetness-Index	DWI	Combined drought index ranging between 0 (*very dry*) and 6 (*very wet*)	—
Growing season net ecosystem production	N_T	Sum of daily NEP between SOS and September (30 September/DOY: 274)	g C m^{-2}
Growing season gross primary production, daytime method	GD_T	Sum of daily GPP:DT between SOS and September (30 September/DOY: 274)	g C m^{-2}
Growing season gross primary production, nighttime method	GN_T	Sum of daily GPP:NT between SOS and September (30 September/DOY: 274)	g C m^{-2}
Growing season first half net ecosystem production	N_1	Sum of daily NEP in April, May, and June	g C m^{-2}
Growing season second half net ecosystem production	N_2	Sum of daily NEP in July, August, and September	g C m^{-2}
Growing season first half gross primary production, daytime method	GD_1	Sum of daily GPP:DT in April, May and June	g C m^{-2}
Growing season second half gross primary production, daytime method	GD_2	Sum of daily GPP:DT in July, August, and September	g C m^{-2}
Growing season first half gross primary production, nighttime method	GN_1	Sum of daily GPP:NT in April, May and June	g C m^{-2}
Growing season second half gross primary production, nighttime method	GN_2	Sum of daily GPP:NT in July, August, and September	g C m^{-2}

the same predictor groups led to similar results, which is why they are not shown here.

Following Zohner et al. (2023), who identify pre-solstice vegetation activity/temperature and autumn temperature as the main drivers of autumn phenology, two additional analyses were performed. First, for each derivation methodology, a multiple linear regression was calculated with the respective EOS as the dependent variable and growing season first half-NEP (N_1) and autumn temperature (T_{AU}) as predictors. Using the median of one predictor variable and the dynamic variable of the other predictor, regression lines were then calculated for the respective methodology.

To gain a better understanding of the interaction of autumn temperature and NEP, particularly in extreme years, we dissected the observed period (2000–2020; 21 years) into all possible combinations of these two variables: years with low T_{AU} and N_1 (scenario 1), high T_{AU} and N_1 (scenario 2), low T_{AU} and high N_1 (scenario 3), and high T_{AU} and low N_1 (scenario 4). To ensure comparability, 5 years were allocated to each scenario as follows: The 10 years with the lowest or highest photosynthetic activity in the first half of the growing season (according to N_1) were determined, excluding the median N_1 year. Within these 10-year subgroups, the 5 years with the coldest or warmest autumn temperatures (by T_{AU})

were then selected. Remarkably, the reverse classification order (first by T_{AU} then by N_1) yielded almost identical results. Finally, for each of the four 5-year subgroups, the mean EOS for each derivation methodology was determined and compared to each other. The general workflow of this study is shown in Figure 2. All relevant work steps were carried out in R (version 4.2.1; R Core Team, 2022).

3 | RESULTS

3.1 | Spring and autumn phenology

Mean SOS in the Hainich National Park started between the beginning of April (94.6; MODIS:GU) and mid-May (134.1; CC:Fraxinus), depending on the source of data (see Figure 3 and Table S2). The single SOS metrics exhibited strong year-to-year fluctuations (SDs) between 5.75 (DWD:LU) and 11.48 (GPP:NT) days. The earliest SOS in the observation period was recorded in mid-March 2019 (DOY 69; GPP:NT), the latest in late May 2017 (DOY 145; CC:Fraxinus; Figure 4). The linear SOS trends from 2000 to 2020 mostly indicated advancing onset dates (−0.23 to −0.78 days per year), and even a statistically significant trend for MODIS:GU. A clear exception is the SOS for ash observed via CC (CC:Fraxinus), which showed a significant positive, that is delayed, trend of 0.82 days per year. It is also worth noting that metrices from indirect derivation methods (MODIS/GPP) are more likely to indicate spring phenology earlier than those from direct methods (DWD/CC).

Comparing the SOS of different data sources, the large range of values was striking (Figure 4): In some extreme years, the difference between individual data sources was more than 70 days, and in general, the SOS values diverged by almost 40 days. The earliest values were detected on average by MODIS (Greenup data, MODIS:GU), usually followed by GPP data. The mean onset dates of DWD, NEP, and MODIS:MGU data, as well as the CC data of the beech (CC:Fagus) were similar and highly correlated (Figure S1). The latest SOS was usually observed for the ash tree via CC (CC:Fraxinus), which was less well correlated with the other SOS variables, such as GPP:DT and GPP:NT.

The mean start of autumn phenology (2000–2020) in the Hainich National Park ranged from the beginning of October (DWD:LC, MODIS:SE) to the beginning of November (MODIS:DO) for the period from 2000 to 2020 (Figure 3 and Table S3). Unlike spring phenology, the variation between individual years was smaller and ranged from 3.09 to 11.09 days SD. The earliest recorded autumn phenology was in late September 2004 (DOY 268; CC:Fagus) and the latest in mid-November 2009 (DOY 320; MODIS:DO; Figure 5). The linear trends from 2000 to 2020 were by far not as clear for autumn as for spring phenology: Six of nine data sources indicated a weak delay (0.06–0.94 days per year), and three data sources indicated a weak trend towards earliness (−0.10 to −0.26 days per year). None of the autumn trends was statistically significant.

A comparison between the individual data sources of autumn phenology also showed extreme differences in the annual range of values, mostly between 30 and 40 days (Figure 5). The senescence detected by MODIS and DWD data usually was at the start of autumn, followed by CC and flux tower data. Autumn ended with DWD leaf fall (DWD:LF) and the subsequent dormancy by MODIS (MODIS:DO). Thus, a clear temporal separation of the two main phases of autumn phenology, leaf discoloration and leaf fall, could be observed with derivation methods that measure these specifically (DWD/MODIS). Derivation methods that did not imply this differentiation (GPP/NEP/CC) are settled in between. Compared to spring phenology, there was even a larger agreement in EOS variables, as indicated by correlation coefficients (Figure S2).

3.2 | Drivers of autumn phenology

Spring phenology correlated only weakly with EOS ($r_s = -.28–.19$, not significant), depending on the data source (Figure 6). Temperature-related explanatory variables, such as summer ($r_s = -.06–.62$, not

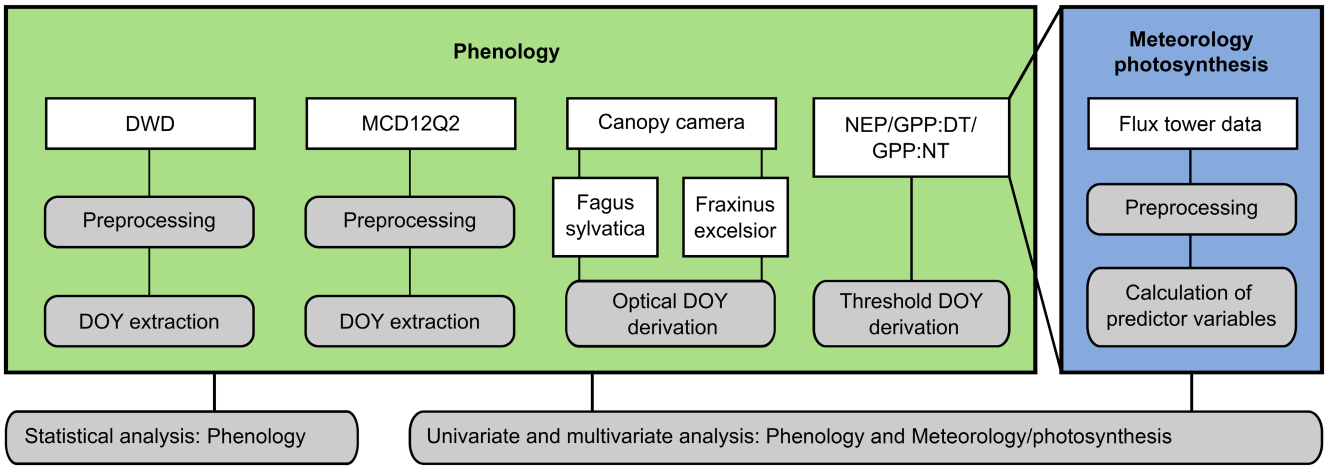

FIGURE 2 Flowchart of used data sources (white boxes) and applied methodology (grey boxes). The main aim is to relate plant phenology data (green box) and meteorological or ecosystem CO_2 exchange-related data (blue box).

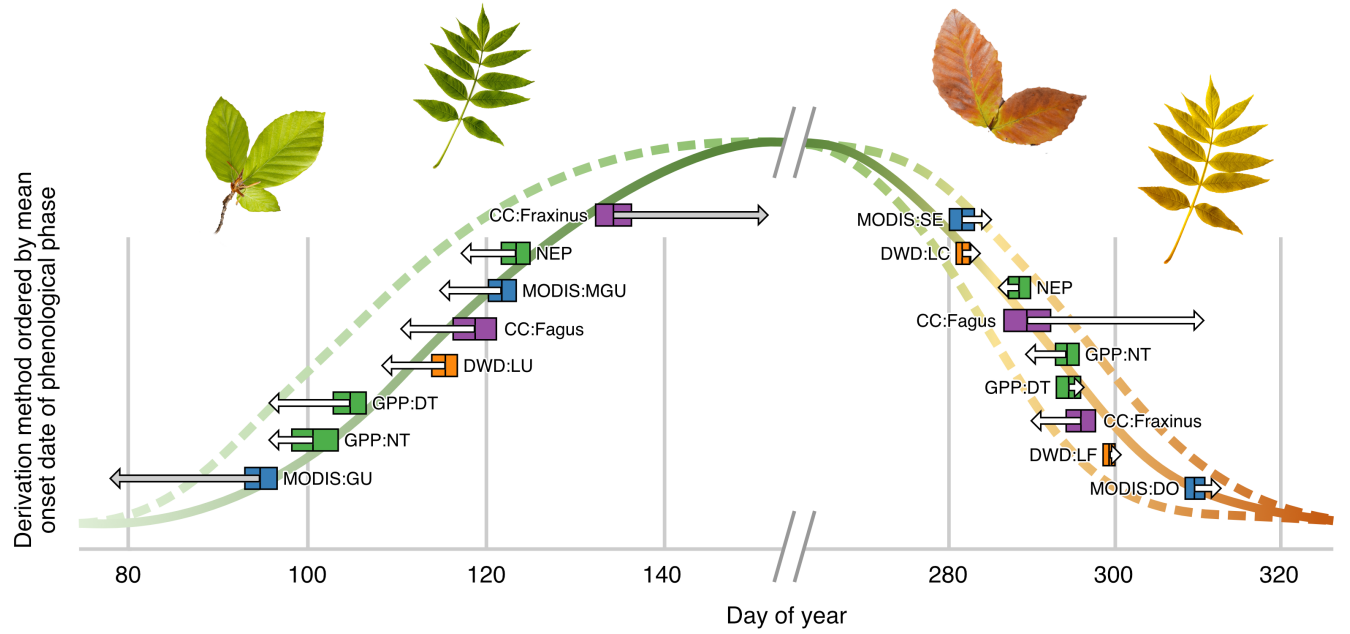

FIGURE 3 Schematic representation of the descriptive statistics of spring and autumn phenology from 2000 to 2020 for the respective data sources (orange: in-situ observation; blue: satellite remote sensing; green: flux tower; purple: canopy camera), ordered by mean DOY. The middle line within each box indicates the mean, the outer boundaries ±one SD. The arrows represent the trends over the observation period of 21 years, with gray coloring indicating statistical significance ($p < .05$). The dashed lines correspond to possible (extrapolated) future trends based on the arrows. The exact values of means, SD and trends are summarized in Tables S2 and S3.

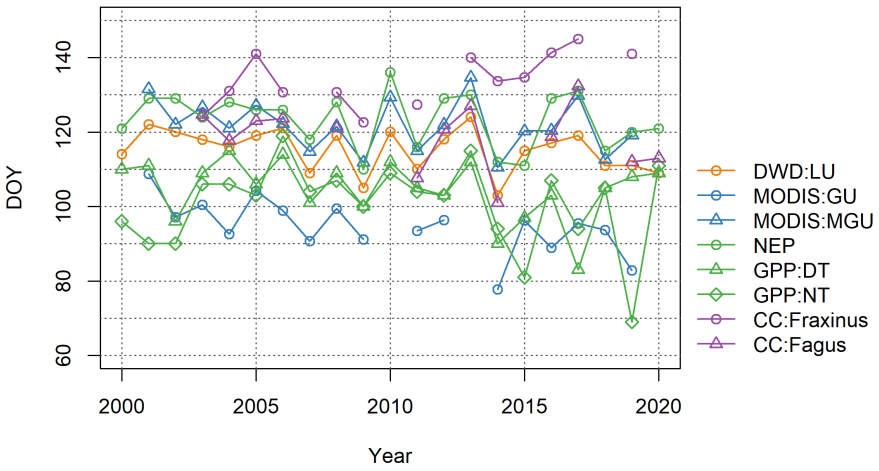

FIGURE 4 Time series of the derived spring phenology from the different data sources (orange: in-situ observation; blue: satellite remote sensing; green: flux tower; purple: canopy camera) in the Hainich National Park from 2000 to 2020.

significant) or autumn temperature ($r_s = .09–.33$, not significant), as well as extreme heat days ($r_s = .04–.64$, not significant), correlated mostly positively for the EOS, indicating that under warm/hot conditions in summer or assessed by extreme heat days, EOS should be observed later. Throughout positive correlations could also be seen for annual frost days ($r_s = .02–.55$, not significant; i.e., frosty winters should be linked to later EOS in autumn). In contrast, spring frost gave ambiguous results depending on the data source ($r_s = -.16–.32$, not significant).

The different variables of water availability had an evident (and sometimes significant) influence on autumn phenology: The less water—be it defined by precipitation in the hydrological year ($r_s = -.76–.08$) or during summer ($r_s = -.69–.05$), by VPD ($r_s = -.52$ to $-.02$, not significant) or DWI ($r_s = -.58$ to $-.18$, not significant)—was available, the later EOS took place (significant: $r_s = -.76$ and p-value $= .0007$ for P_{HY} and CC:Fagus; $r_s = -.67$ and p-value $= .0046$ for P_{SU} and CC:Fagus).

The variables of ecosystem CO_2 exchange provided a differentiated picture: The lower the NEP or GPP (and correspondingly less CO_2 uptake), the later EOS usually was. These effects were especially pronounced for the entire and the second half of the growing season and the NEP/GPP:NT explanatory variables ($r_s = -.60–.31$, not significant). In contrast, regarding the variables concerning the first half of the annual growth period (N_1, GD_1, GN_1), the correlations with the EOS were more spread, including positive and negative associations depending on the data source ($r_s = -.39–.51$, not significant).

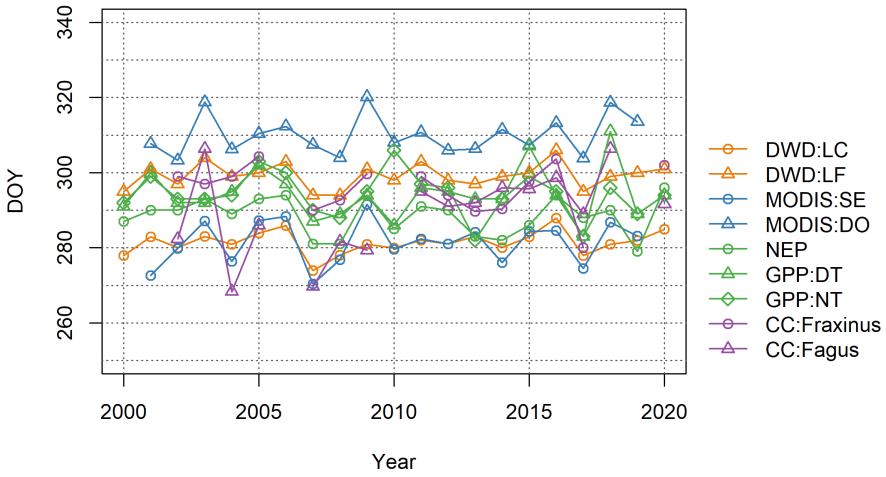

FIGURE 5 Time series of the derived autumn phenology from the different data sources (orange: in-situ observation; blue: satellite remote sensing; green: flux tower; purple: canopy camera) in the Hainich National Park from 2000 to 2020.

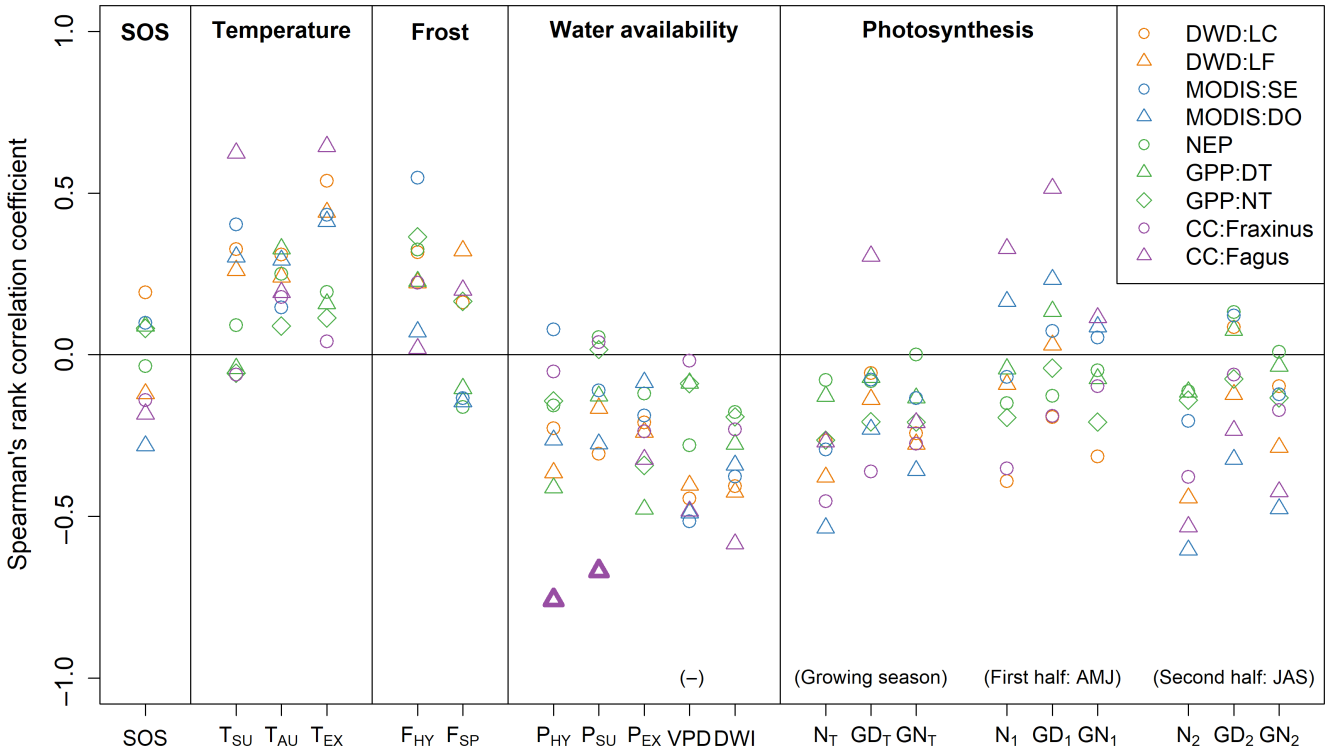

FIGURE 6 Spearman's rank correlation coefficient between the derived EOS and the respective predictor (variables see Table 1). Positive correlations indicate a delay in the EOS, while negative correlations mean an advance in EOS if the amount of the respective variable increases. To simplify the interpretation of the graph, the sign of VPD (−) has been changed (high VPD therefore means humid conditions). Symbols marked in bold represent a statistically significant correlation ($p < .05$, Bonferroni corrected).

If only the direct methods (DWD and CC) are considered in this respect, a similar picture emerges: While spring phenology and photosynthetic activity in April, May, and June indicate an ambiguous influence, higher temperatures in summer and autumn, more frost days, drier conditions, and lower photosynthetic activity in the growing season and in July, August, and September are associated with a later EOS.

This general variance in the sign and/or strength of correlation coefficients depending on the data source and variable was striking (Figure 6; e.g., summer temperature or precipitation). Among the phenological metrics, in-situ, CC, and remote sensing approaches tended to display stronger correlation coefficients (except T_{AU} and P_{EX}) than flux-related ones (NEP, GPP:DT, GPP:NT). Differences between direct (DWD/CC) and indirect (MODIS/GPP/NEP) derivation methodologies and between early (DWD:LC/MODIS:SE) and late autumn phenological (DWD:LF/MODIS:DO) metrics could not be detected in the univariate analysis.

In the multivariate analysis, the results of the univariate analyses were mostly confirmed (Figure 7 and Figures S3–S5). In the combination of the predictors from the groups of temperature, precipitation and photosynthesis, an increased autumn temperature and, in some cases, an increased summer temperature had an EOS-delaying

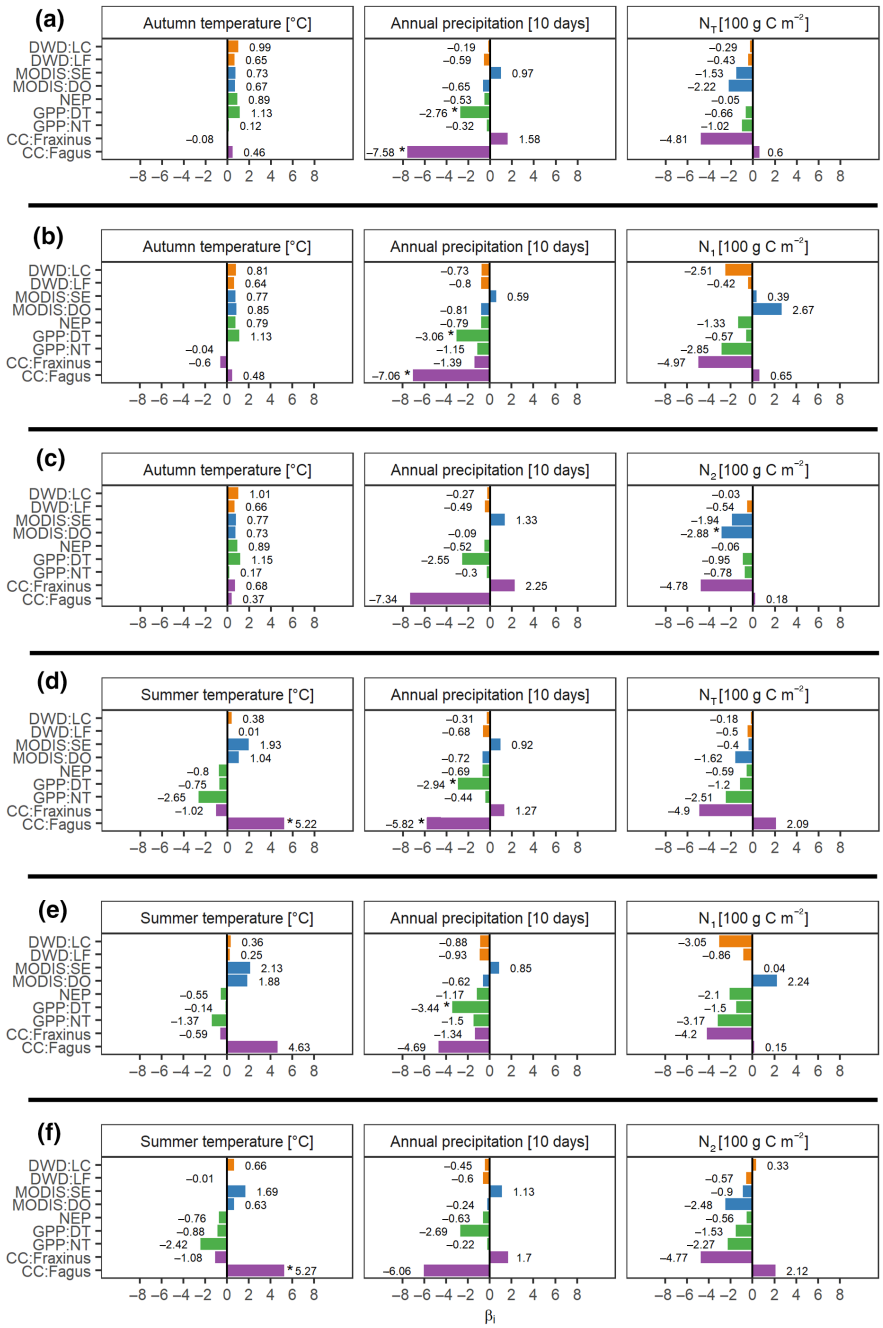

FIGURE 7 Regression coefficients of the respective predictor variable within the linear multiple regression models between EOS metrics and (a) T_{AU}, P_{HY}, and N_T; (b) T_{AU}, P_{HY}, and N_1; (c) T_{AU}, P_{HY}, and N_2; (d) T_{SU}, P_{HY}, and N_T; (e) T_{SU}, P_{HY}, and N_1; (f) T_{SU}, P_{HY}, and N_2. Statistically significant ($p < .05$) regression coefficients are marked with an asterisk.

effect. In contrast, wetter conditions and increased photosynthetic activity over the entire vegetation period and in the second half (July/August/September) had an advancing effect on the EOS, while photosynthetic activity in the first half of the vegetation period (April/May/June) showed diverging results depending on the data source. This also applies if only the direct methods (CC and DWD) are considered, except for photosynthetic activity in the first half of the growing season (the higher, the earlier EOS).

In general, the data source significantly influenced the sign, magnitude, and significance of the regression coefficient of the multiple linear regression models. This also became clear in the key statistics of the individual models (Table 2): With the identical predictor data set and only changing EOS data source, R^2 (.03–.62), adjusted R^2 (−.17–.52) and p-value (.01–.91) varied considerably. As in the univariate analysis, differences between direct (DWD/CC) and indirect (MODIS/GPP/NEP) derivation methodologies and between early (DWD:LC/MODIS:SE) and late autumn phenological (DWD:LF/MODIS:DO) metrics could not be detected.

The data source played a crucial role in investigating the interplay between EOS, N_1, and T_{AU}, as proposed by Zohner et al. (2023). When keeping autumn temperature constant, the various EOS responses showed a nuanced pattern relative to N_1 (Figure 8a): While higher photosynthetic activity in the first half of the growing season lead to a delay in the autumn phenology of GPP:DT, MODIS:DO, and especially CC:Fagus, some of the EOS variables were hardly affected, or even occurred earlier (CC:Fraxinus, GPP:NT, and DWD:LC). Conversely, under stable N_1 conditions, a rise in autumn temperature predominantly resulted in delayed EOS (except CC:Fraxinus and GPP:NT).

TABLE 2 Statistical ratios (coefficient of determination, adjusted coefficient of determination and *p*-value) of the multiple linear models between the respective EOS and the three predictor variable variants (see Figure 7).

	Variable combination	Statistical ratio	DWD: LC	DWD: LF	MODIS: SE	MODIS: DO	NEP	GPP: DT	GPP: NT	CC: Fraxinus	CC: Fagus
(a)	T_{AU}	R^2	.21	.18	.10	.30	.07	.34	.05	.29	.46
	P_{HY}	R^2 (adj.)	.06	.03	−.08	.16	−.10	.22	−.13	.10	.32
	N_T	*p*-value	.27	.34	.67	.14	.74	.07	.84	.26	.05
(b)	T_{AU}	R^2	.30	.17	.03	.16	.08	.34	.05	.08	.46
	P_{HY}	R^2 (adj.)	.17	.01	−.16	.00	−.09	.21	−.13	−.17	.32
	N_1	*p*-value	.11	.39	.91	.43	.69	.08	.83	.80	.05
(c)	T_{AU}	R^2	.20	.19	.13	.40	.07	.35	.03	.23	.46
	P_{HY}	R^2 (adj.)	.05	.04	−.04	.28	−.10	.23	−.15	.02	.32
	N_2	*p*-value	.29	.33	.54	.04	.74	.07	.91	.39	.05
(d)	T_{SU}	R^2	.06	.12	.15	.30	.04	.31	.19	.31	.62
	P_{HY}	R^2 (adj.)	−.12	−.05	−.02	.16	−.14	.18	.04	.12	.52
	N_T	*p*-value	.81	.56	.46	.14	.87	.11	.32	.23	.01
(e)	T_{SU}	R^2	.21	.11	.15	.26	.06	.29	.11	.08	.59
	P_{HY}	R^2 (adj.)	.07	−.06	−.02	.12	−.12	.16	−.06	−.17	.49
	N_1	*p*-value	.27	.58	.47	.19	.79	.13	.60	.81	.01
(f)	T_{SU}	R^2	.06	.12	.17	.38	.04	.32	.15	.24	.61
	P_{HY}	R^2 (adj.)	−.11	−.05	.00	.25	−.14	.19	−.01	.03	.52
	N_2	*p*-value	.79	.53	.42	.06	.88	.10	.44	.38	.01

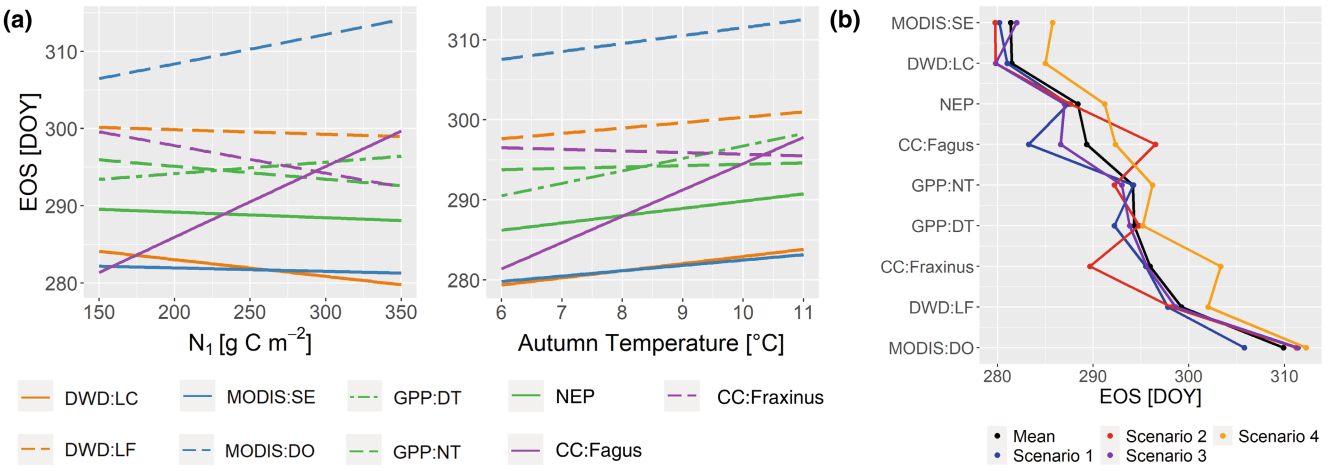

FIGURE 8 Analysis of EOS metrics in combination with the predictor variables autumn temperature (T_{AU}) and growing season first half net ecosystem production (N_1): (a) Multiple linear regressions with the other variable kept constant (median); (b) mean EOS (metrics ordered by mean date of onset), for 5 years each with low T_{AU} and N_1 (scenario 1), with high T_{AU} and N_1 (scenario 2), with low T_{AU} and high N_1 (scenario 3), with high T_{AU} and low N_1 (scenario 4), and for the total period (mean).

When comparing four 5-year scenarios across the EOS metrics (Figure 8b), it is most noticeable that in years with low photosynthetic activity in the first half of the growing season and high autumn temperature at the same time, a delayed EOS is observed in most of the methodologies. All other scenarios behave differently depending on the methodology, but the EOS values are always close to each other. In both analyses, no differences were observed between direct/indirect and early and late autumn phenological metrics.

4 | DISCUSSION

Both spring and autumn phenology in the Hainich National Park over the last 20 years differed widely by up to 1.5 months when different sources of derivation, such as remote sensing, carbon fluxes, CC images, or in-situ observations, are considered. However, the resulting time series still had remarkable similarities in their temporal courses. Whereas there is largely consensus that spring phenology in temperate deciduous forests is mainly driven by spring temperatures (besides winter chilling and photoperiod), the drivers of autumn phenology are less clear and heavily debated (e.g., Lu & Keenan, 2022). Consequently, our main intention was to analyze whether EOS data sources influence analyses' outcome on autumn phenology drivers, such as temperature, water availability, and/or photosynthetic activity. In the following sections, we will discuss the considerable differences found between the data sources and their implications for predicting changes in the growing season length of deciduous forests under climate change.

4.1 | Spring and autumn phenology

Spring phenology metrics from different data sources, such as satellite remote sensing, carbon flux data, CC, and in-situ observations, are well-known to differ (Berra & Gaulton, 2021). However, their seasonal order seems not random but well justified by inherent properties of the different indices. The MODIS Greenup, with its low threshold of 15% of EVI2 amplitude, mainly focuses on the greening of understory vegetation such as *Allium ursinum* L., *Mercurialis perennis* L., *Anemone nemorosa* L., usually occurring earlier in the year than the greening of the overstory (Filippa et al., 2018; Ryu et al., 2014; Uphus et al., 2021). Equally, the flux tower phenology also partially records the photosynthetic activity of the understory, leading to earlier GPP-based SOS dates (D'Odorico et al., 2015), albeit slightly later than MODIS:GU. This difference can be interpreted to signify as meaning that the greening of understory vegetation occurs before any relevant carbon uptake processes are initiated. The observation that indirect derivation methods are the first to indicate the start of spring phenology, compared to direct methods observing the trees themselves can therefore be primarily explained by the recording of the understory, which shows a clear drawback of the recording method. Unsurprisingly, the CC and the interpolated DWD phenology of *F. sylvatica* largely match. Corresponding to literature findings (Ahrends et al., 2009; Smith & Ramsay, 2020) *F. excelsior* leaves out later than *F. sylvatica*.

Advancing trends of SOS in the Hainich National Park from 2000 to 2020 are predominantly in line with the current literature (Caparros-Santiago et al., 2021; Menzel et al., 2020; Piao et al., 2019) and are mainly caused by rising spring temperatures (Hamunyela et al., 2013; Jin et al., 2019). On the contrary, the statistically significant delay of *F. excelsior* SOS might be a consequence of the pathogenic fungus *Hymenoscyphus pseudoalbidus*, which is currently damaging ash trees across Europe (Kowalski & Holdenrieder, 2009; but then Queloz et al., 2011). This phenomenon is also increasingly observed in the Hainich National Park. More severely damaged trees tend to leave out later than healthy ones (McKinney et al., 2011; Stener, 2013). These results highlight that "ecosystem-scale" indirect approaches are not very reliable in addressing species-specific phenology trends and could lead to large errors for species experiencing a phenological shift that is

inverse to the other plants in the community. Furthermore, since SOS dates are often used as predictors for EOS onset dates (assuming a constant length of the growing season; for example, Keenan & Richardson, 2015; Liu, Fu, Zhu, et al., 2016), it is essential to note that all SOS data sources, except for the ash CC, show similarly inter-annually varying time series and have a similar range (e.g., MODIS:MGU, DWD:LU, NEP, CC:Fagus). This indicates that for this specific assumed driver of EOS, differences in SOS metrics should not play a major role.

In autumn, as in spring, the order of the determined phenology was in line with the current process understanding. The data sources that explicitly detect the beginning of autumn phenology—namely leaf discoloration—(DWD:LC and MODIS:SE) estimated the earliest onset dates on average. The data sources indicating a later EOS were related to leaf fall (DWD:LF and MODIS:DO), with the MODIS data occurring significantly later (over 10 days on average).

The other autumn phenology metrics had a similar range of values in between, whereby two points are particularly noteworthy: Firstly, the DWD:LC data (which are based on 50% leaf discoloration of *F. sylvatica*) were more than 1 week earlier than CC:Fagus, although by definition the same is measured—in the top canopy (CC) and from the ground (DWD). This lag of 1 week could be because the phenological variability of individual trees is quite large and differences within certain phenological phases of more than 7 days are not uncommon (Capdevielle-Vargas et al., 2015; Marchand et al., 2020). Moreover, the DWD data are interpolated data, which per se represents an uncertainty factor, and thus can explain these differences. The Hainich site is slightly elevated to the Thuringen Becken, so it could be that the interpolation does not capture properly the elevational effect at this site. Secondly, ash leaf discoloration or leaf fall was later than the corresponding autumn phenology of beech, as also reported by Ahrends et al. (2009) for the Hainich National Park. The CC analysis clearly showed the dissimilarity: While *F. sylvatica* has intensive leaf discoloration and both leaf discoloration and leaf fall are longer lasting processes, the leaves of *F. excelsior* hardly change color and then fall to the ground relatively abruptly.

The autumn phenological trends across different data sources were rather delayed than advanced (but no single significant trend in either direction). This aligns well with existing research (Gill et al., 2015; Piao et al., 2019), although no directly comparable study with a similar observation period and area is available. Another striking difference is the sign of the two species observed via the CC. While the ash tends to enter dormancy earlier, the phenological autumn of the beech is clearly delayed. Contrasting the results of McKinney et al. (2011) and Stener (2013), we assume an influence of ash dieback also on the autumn phenology, which can be seen due to an advance in leaf senescence. The observed differences can be justified here based on a different research area, method, and period. In summary, there were thus two opposing trends in the length of the growing season for the Hainich National Park: a lengthening for *F. sylvatica* and a shortening for *F. excelsior*. Despite the high variance of the individual data sources in the value range of EOS, there is a high degree of temporal agreement. Above all, DWD:LC, DWD:LF, MODIS:SE, NEP and CC:Fraxinus show similar temporal courses and thus form a solid EOS construct for the Hainich National Park.

4.2 | Predictor analysis of autumn phenology

The predictor analysis of autumn phenology revealed that spring phenology, spring frost, and (partly) summer temperatures exhibit minor or contradicting effects—depending on the data source for autumn phenology. However, years with higher autumn (and partly summer) temperatures and more heat and frost days tend to be associated with a later EOS. These outcomes hold a dual nature, aligning with some and diverging from other research findings. While many studies support the idea that higher autumn temperatures cause leaves to change color and fall later (e.g., Gallinat et al., 2015; Gill et al., 2015; Zohner et al., 2023), there are some studies that do not offer evidence for a later EOS with higher summer temperatures (Liu et al., 2018; Lu & Keenan, 2022). However, a noteworthy discrepancy arises concerning our consistently positive link between the number of extreme hot days and the EOS, that is more hot days are associated with later autumn senescence contrasting with results of Xie et al. (2015, 2018) who associate extreme heat stress with an earlier autumn phenology. This discrepancy could be due to the methodology: Xie et al. (2015) analyzed remote sensing data in the US from 2001 to 2012, defining heat stress in July and August as temperatures exceeding 32 or 35°C, whereas Xie et al. (2018) also considered ground observations with a threshold of 35°C. Their findings on the relationship between heat stress and EOS changed depending on the threshold (Xie et al., 2015) and tree species (Xie et al., 2018), which is in agreement with our results. Consequently, there is a need to further investigate in detail whether higher temperature thresholds than applied in our study lead to the detection of possible drought effects associated with heat waves in remote sensing products, resulting in this reverse relationship with EOS.

A clear influence was seen for water availability: the less precipitation falls in the previous hydrological year, in summer, and as extremes, the later the autumn phenology. This finding was also confirmed for VPD and DWI influences in our study. When considering the impact of water availability, some studies observe a later EOS in drier conditions (Xie et al., 2015, 2018), although other studies cannot confirm this finding (Bigler & Vitasse, 2021; Liu et al., 2018; Zani et al., 2020). In general, the understanding of this topic is still unclear, since there are many different variables (e.g., precipitation, soil moisture, VPD) and methods (mean values or extremes) involved.

The impact of photosynthetic activity on EOS requires a more differentiated assessment, particularly given the conflicting statements in current literature. While some studies support the idea that photosynthetic activity regulates autumn phenology (Zani et al., 2020; Zohner et al., 2023), others oppose this hypothesis (Lu & Keenan, 2022; Norby, 2021). We found that the effect for the first part of the growing season varied based on how EOS is determined, and the analysis method used (univariate/multivariate). This was equally the case, when only photosynthetic activity in the first half

of the growing season and autumn temperature were considered as predictor variables. On the other hand, reduced photosynthetic activity over the entire growing season and in the second half of the season (July, August, September) was more likely to delay EOS. Nevertheless, the dominating effect was autumn temperature, with a high temperature being associated with a later EOS in most cases. Consequently, years with low photosynthesis in April, May, and June and high autumn temperature were particularly associated with delayed EOS, indicating the autumn temperature effect. However, in detail this was again true not for all EOS data sources and the photosynthesis definition (NEP, GPP) influenced the results significantly.

Recent results by Zohner et al. (2023), according to which increased pre-solstice vegetation activity advances senescence in Northern Hemisphere forests, cannot be confirmed by our study. EOS metrics determined the overall picture and the phases specifically related to the beginning of senescence (e.g., MODIS:SE and DWD:LC) provided different results, which makes this hypothesis questionable, at least in a temperate mid-latitude deciduous forest.

One finding is valid for all influencing factors: the different data sources for phenology matter. Although some studies already link derived autumn phenology with potential predictors using different data sources and methodologies (e.g., Keenan & Richardson, 2015; Lu & Keenan, 2022), to our knowledge, there is no systematic evaluation of how different derivation approaches of EOS affect a predictor analysis in a given study area. We found large differences in the magnitude, sign, and significance of effects on autumn phenology depending on the data source and derivation methodology. For example, beech CC EOS dates were highly correlated with temperature and water variables, suggesting a strong relationship, whereas correlations for the same variables were much weaker or even opposite for flux tower phenology. Similar observations can be made at the multivariate level, where, for example, the NEP, GPP, and ash CC autumn phenology were negatively related to summer temperature. In contrast, the DWD and MODIS phenology showed (mostly) a positive correlation. Both examples illustrate that conclusions about drivers of autumn phenology can diverge considerably depending on the data source. This finding is noteworthy, as many studies within this field of research base statements about relationships between phenology and possible influencing factors on only one data source and derivation methodology. On the other hand, however, it must also be noted that despite the large number of different data sources and derivation methods, the correlations in the more general variable groups (temperature, water availability, photosynthesis) with the EOS variables provide a largely uniform picture. There were no discernible structural differences in the relationships with the individual predictor variables found either in the differentiation between direct and indirect recording methods or in early, mid-, and late autumn phenological metrics.

However, the choice of methods can lead to substantial variations in EOS-related findings (especially just looking at one predictor variable), whereby for general statements on potential predictors of autumn phenology, an ensemble evaluation of all available data sources of a study area is recommendable but requires considerably larger data sets. In the context of machine learning ensemble analysis, the fundamental premise is that inherent inaccuracies of individual models can be mitigated through the combination of multiple models. This approach is expected to enhance predictive accuracy compared to relying on single models (Sagi & Rokach, 2018). In our specific context, where various phenological data sources or derivation methods were employed for a given location and observation period to analyze phenological trends and their drivers, we constructed several regression models using a singular model type. Thus, this above-mentioned methodology would open up new avenues, particularly for extensive phenological data sets which amalgamate diverse data sources. However, ensemble methods from the field of machine learning, such as boosting (Elith et al., 2008) and bagging (Breiman, 1996), have not yet received much attention in plant phenology but hold potential for refining models for various research questions. Nevertheless, for differentiated views, especially concerning spatial resolution (ecosystem, species, individual tree, etc.), individual data sources still have importance for specific applications.

In light of our study findings, it is evident across all EOS metrics that warmer and drier growing seasons lead to a later EOS. At the same time, cooler and wetter conditions tend to prompt an earlier EOS in the Hainich National Park, with the role of photosynthetic activity remaining unclear, contingent on the definition, observation period, and EOS methodology.

4.3 | Limitations of the data sources

However, there are also specific limitations related to the data and methods. Only individual trees of the respective species were observed by DWD and CC data. As previously mentioned, there can be substantial variability within a phenological phase among trees (Capdevielle-Vargas et al., 2015; Marchand et al., 2020), and thus, in the worst case, the determined phenological phase might not accurately represent the species studied. The interpolation of DWD data adds another layer of uncertainty. Particularly worth noting is the manual and, thus semi-objective nature of evaluating phenology in the case of the CC data. Also, since the camera position changed several times over the time series, the same tree was not always observed consistently. In the case of the remote sensing and flux tower data, the homogeneous and spatially undifferentiated observation must be pointed out, which can lead to distorted results, especially in respect to the understory. Across all data sources and phenology studies (Berra & Gaulton, 2021; Templ et al., 2018; Zeng et al., 2020), there is also concern about consistent definitions of the phenological phases. Especially in autumn, due to the more complex process of leaf discoloration and fall, phenology can be measured differently. Additionally, indirect measurement methods such as remote sensing or derivation via ecosystem CO_2 exchange, can sometimes lack clarity in terms of what exactly is being measured, making comparisons challenging. For eddy covariance data, uncertainties arise from quality checks, gap-filling, and the source partitioning approach. Finally, GPP:DT and GPP:NT are just modelled values; only NEP is directly measured. Uncertainties also extend to the predictor variables. The

defined threshold values and the periods can be designed differently, influencing evaluations. However, careful selection of robust variables was prioritized when avoiding collinearity within the multiple linear regression models. Lastly, the limitations of the statistical analyses conducted here should be acknowledged. The dataset size (maximum 21 years) upon which the statistical metrics are based was relatively small, making it sensitive to outliers.

5 | CONCLUSION

The analysis of spring and autumn phenology in the Hainich National Park from different data sources revealed significant variability in the determined onset dates and corresponding trends, dependent on the specific data source employed. While spring phenology generally exhibited advancement over the observed period (except for European ash), autumn trends were less distinct, aside from the delayed leaf coloring in European beech. The factors possibly influencing autumn phenology include temperature, water availability, and/or photosynthetic activity. Warmer and drier years tend to be linked to a delayed end of season, although the exact role of photosynthesis remains unclear. Notably, the predictors derived for autumn phenology exhibit substantial disparities across the EOS data sources, whereby no structural differences are found between direct and indirect data sources or between early and late autumn phenological metrics. Considering these findings, it appears prudent to adopt an ensemble approach by using multiple phenological data sources in future research, particularly when addressing broader questions concerning plant phenology.

AUTHOR CONTRIBUTIONS

Simon Kloos: Conceptualization; data curation; formal analysis; investigation; methodology; software; validation; visualization; writing – original draft; writing – review and editing. **Anne Klosterhalfen:** Data curation; investigation; resources; writing – review and editing. **Alexander Knohl:** Data curation; funding acquisition; project administration; resources; writing – review and editing. **Annette Menzel:** Conceptualization; funding acquisition; methodology; project administration; supervision; writing – review and editing.

ACKNOWLEDGMENTS

The authors thank the Land Processes Distributed Active Archive Center (LP DAAC), the DWD Climate Data Center (CDC), and the Integrated Carbon Observation System (ICOS) data portal for providing the data free of charge. We thank the technical staff from the Bioclimatology Group of the University of Göttingen for their continuous support in data acquisition and instrument maintenance and Matthias Neumair and Donna P. Ankerst for statistical advice. Thanks also go to Johanna Kauffert and Lars Uphus for manually determining the CC phenology. Finally, we thank the administration of the Hainich National Park for the opportunity for research within the National Park. Open Access funding enabled and organized by Projekt DEAL.

FUNDING INFORMATION

This study was performed within the project BAYSICS (Bavarian Citizen Science Portal for Climate Research and Science Communication), funded by the Bavarian State Ministry of Science and the Arts in the context of the Bavarian Climate Research Network (bayklif). We acknowledge support by the German Federal Ministry of Education and Research (BMBF) as part of the European Integrated Carbon Observation System (ICOS), by the Deutsche Forschungsgemeinschaft (INST 186/1118-1 FUGG), and the Digital Forest project funded by Niedersächsisches Vorab (ZN 3679), Ministry of Lower-Saxony for Science and Culture (MWK).

CONFLICT OF INTEREST STATEMENT

The authors declare no conflicts of interest.

DATA AVAILABILITY STATEMENT

The phenological data that support the findings of this study are openly available in figshare at https://doi.org/10.6084/m9.figshare.22040828, the DWD data are publicly available at https://opendata.dwd.de/climate_environment/CDC/grids_germany/annual/phenology/ (RBUBO, RBUBV, and RBUBF), the flux tower data are openly available in the ICOS data portal at https://doi.org/10.18160/cr66-pj24, and the MODIS data were downloaded with the R package MODIStsp (Busetto & Ranghetti, 2016). The canopy camera images are publicly available at https://doi.org/10.25625/6IWFIY.

ORCID

Simon Kloos https://orcid.org/0000-0002-9242-1456
Anne Klosterhalfen https://orcid.org/0000-0001-7999-8966
Alexander Knohl https://orcid.org/0000-0002-7615-8870
Annette Menzel https://orcid.org/0000-0002-7175-2512

REFERENCES

Ahrends, H. E., Etzold, S., Kutsch, W. L., Stoeckli, R., Bruegger, R., Jeanneret, F., Wanner, H., Buchmann, N., & Eugster, W. (2009). Tree phenology and carbon dioxide fluxes: Use of digital photography for process-based interpretation at the ecosystem scale. *Climate Research*, *39*, 261–274. https://doi.org/10.3354/cr00811

Barnard, D. M., Knowles, J. F., Barnard, H. R., Goulden, M. L., Hu, J., Litvak, M. E., & Molotch, N. P. (2018). Reevaluating growing season length controls on net ecosystem production in evergreen conifer forests. *Scientific Reports*, *8*(1), 17973. https://doi.org/10.1038/s41598-018-36065-0

Berra, E. F., & Gaulton, R. (2021). Remote sensing of temperate and boreal forest phenology: A review of progress, challenges and opportunities in the intercomparison of in-situ and satellite phenological metrics. *Forest Ecology and Management*, *480*, 118663. https://doi.org/10.1016/j.foreco.2020.118663

Bigler, C., & Vitasse, Y. (2021). Premature leaf discoloration of European deciduous trees is caused by drought and heat in late spring and cold spells in early fall. *Agricultural and Forest Meteorology*, *307*, 108492. https://doi.org/10.1016/j.agrformet.2021.108492

Breiman, L. (1996). Bagging predictors. *Machine Learning*, *24*(2), 123–140. https://doi.org/10.1007/BF00058655

Busetto, L., & Ranghetti, L. (2016). MODIStsp: An R package for automatic preprocessing of MODIS land products time series.

Computers & Geosciences, *97*, 40–48. https://doi.org/10.1016/j.cageo.2016.08.020

Caparros-Santiago, J. A., Rodriguez-Galiano, V., & Dash, J. (2021). Land surface phenology as indicator of global terrestrial ecosystem dynamics: A systematic review. *ISPRS Journal of Photogrammetry and Remote Sensing*, *171*, 330–347. https://doi.org/10.1016/j.isprsjprs.2020.11.019

Capdevielle-Vargas, R., Estrella, N., & Menzel, A. (2015). Multiple-year assessment of phenological plasticity within a beech (*Fagus sylvatica* L.) stand in southern Germany. *Agricultural and Forest Meteorology*, *211-212*, 13–22. https://doi.org/10.1016/j.agrformet.2015.03.019

Chen, L., Hänninen, H., Rossi, S., Smith, N. G., Pau, S., Liu, Z., Feng, G., Gao, J., & Liu, J. (2020). Leaf senescence exhibits stronger climatic responses during warm than during cold autumns. *Nature Climate Change*, *10*(8), 777–780. https://doi.org/10.1038/s41558-020-0820-2

D'Odorico, P., Gonsamo, A., Gough, C. M., Bohrer, G., Morison, J., Wilkinson, M., Hanson, P. J., Gianelle, D., Fuentes, J. D., & Buchmann, N. (2015). The match and mismatch between photosynthesis and land surface phenology of deciduous forests. *Agricultural and Forest Meteorology*, *214-215*, 25–38. https://doi.org/10.1016/j.agrformet.2015.07.005

DWD Climate Data Center. (2022). Annual grids of several phenological plant stages in Germany, version 0.x. https://opendata.dwd.de/climate_environment/CDC/grids_germany/annual/phenology/

Elith, J., Leathwick, J. R., & Hastie, T. (2008). A working guide to boosted regression trees. *The Journal of Animal Ecology*, *77*(4), 802–813. https://doi.org/10.1111/j.1365-2656.2008.01390.x

Estrella, N., & Menzel, A. (2006). Responses of leaf colouring in four deciduous tree species to climate and weather in Germany. *Climate Research*, *32*, 253–267. https://doi.org/10.3354/cr032253

Filippa, G., Cremonese, E., Migliavacca, M., Galvagno, M., Sonnentag, O., Humphreys, E., Hufkens, K., Ryu, Y., Verfaillie, J., Di Morra Cella, U., & Richardson, A. D. (2018). NDVI derived from near-infrared-enabled digital cameras: Applicability across different plant functional types. *Agricultural and Forest Meteorology*, *249*, 275–285. https://doi.org/10.1016/j.agrformet.2017.11.003

Fu, Y. H., Piao, S., Delpierre, N., Hao, F., Hänninen, H., Geng, X., Peñuelas, J., Zhang, X., Janssens, I. A., & Campioli, M. (2019). Nutrient availability alters the correlation between spring leaf-out and autumn leaf senescence dates. *Tree Physiology*, *39*(8), 1277–1284. https://doi.org/10.1093/treephys/tpz041

Fu, Y. H., Piao, S., Delpierre, N., Hao, F., Hänninen, H., Liu, Y., Sun, W., Janssens, I. A., & Campioli, M. (2018). Larger temperature response of autumn leaf senescence than spring leaf-out phenology. *Global Change Biology*, *24*(5), 2159–2168. https://doi.org/10.1111/gcb.14021

Gaertner, B. A., Zegre, N., Warner, T., Fernandez, R., He, Y., & Merriam, E. R. (2019). Climate, forest growing season, and evapotranspiration changes in the central Appalachian Mountains, USA. *The Science of the Total Environment*, *650*(Pt 1), 1371–1381. https://doi.org/10.1016/j.scitotenv.2018.09.129

Gallinat, A. S., Primack, R. B., & Wagner, D. L. (2015). Autumn, the neglected season in climate change research. *Trends in Ecology & Evolution*, *30*(3), 169–176. https://doi.org/10.1016/j.tree.2015.01.004

Garonna, I., de Jong, R., & Schaepman, M. E. (2016). Variability and evolution of global land surface phenology over the past three decades (1982-2012). *Global Change Biology*, *22*(4), 1456–1468. https://doi.org/10.1111/gcb.13168

Garrity, S. R., Bohrer, G., Maurer, K. D., Mueller, K. L., Vogel, C. S., & Curtis, P. S. (2011). A comparison of multiple phenology data sources for estimating seasonal transitions in deciduous forest carbon exchange. *Agricultural and Forest Meteorology*, *151*(12), 1741–1752. https://doi.org/10.1016/j.agrformet.2011.07.008

Gill, A. L., Gallinat, A. S., Sanders-DeMott, R., Rigden, A. J., Short Gianotti, D. J., Mantooth, J. A., & Templer, P. H. (2015). Changes in autumn senescence in northern hemisphere deciduous trees: A meta-analysis of autumn phenology studies. *Annals of Botany*, *116*(6), 875–888. https://doi.org/10.1093/aob/mcv055

Gray, J., Sulla-Menashe, D., & Friedl, M. A. (2019). *User guide to collection 6 MODIS land cover dynamics (MCD12Q2) product*. https://lpdaac.usgs.gov/products/mcd12q2v006/

Grossiord, C., Bachofen, C., Gisler, J., Mas, E., Vitasse, Y., & Didion-Gency, M. (2022). Warming may extend tree growing seasons and compensate for reduced carbon uptake during dry periods. *Journal of Ecology*, *110*(7), 1575–1589. https://doi.org/10.1111/1365-2745.13892

Hamunyela, E., Verbesselt, J., Roerink, G., & Herold, M. (2013). Trends in spring phenology of Western European deciduous forests. *Remote Sensing*, *5*(12), 6159–6179. https://doi.org/10.3390/rs5126159

Jin, H., Jönsson, A. M., Bolmgren, K., Langvall, O., & Eklundh, L. (2017). Disentangling remotely-sensed plant phenology and snow seasonality at northern Europe using MODIS and the plant phenology index. *Remote Sensing of Environment*, *198*, 203–212. https://doi.org/10.1016/j.rse.2017.06.015

Jin, H., Jönsson, A. M., Olsson, C., Lindström, J., Jönsson, P., & Eklundh, L. (2019). New satellite-based estimates show significant trends in spring phenology and complex sensitivities to temperature and precipitation at northern European latitudes. *International Journal of Biometeorology*, *63*(6), 763–775. https://doi.org/10.1007/s00484-019-01690-5

Keenan, T. F., Gray, J., Friedl, M. A., Toomey, M., Bohrer, G., Hollinger, D. Y., Munger, J. W., O'Keefe, J., Schmid, H. P., Wing, I. S., Yang, B., & Richardson, A. D. (2014). Net carbon uptake has increased through warming-induced changes in temperate forest phenology. *Nature Climate Change*, *4*(7), 598–604. https://doi.org/10.1038/nclimate2253

Keenan, T. F., & Richardson, A. D. (2015). The timing of autumn senescence is affected by the timing of spring phenology: Implications for predictive models. *Global Change Biology*, *21*(7), 2634–2641. https://doi.org/10.1111/gcb.12890

Kim, J. H., Hwang, T., Yang, Y., Schaaf, C. L., Boose, E., & Munger, J. W. (2018). Warming-induced earlier greenup leads to reduced stream discharge in a temperate mixed forest catchment. *Journal of Geophysical Research: Biogeosciences*, *123*(6), 1960–1975. https://doi.org/10.1029/2018JG004438

Klosterman, S., Melaas, E., Wang, J. A., Martinez, A., Frederick, S., O'Keefe, J., Orwig, D. A., Wang, Z., Sun, Q., Schaaf, C., Friedl, M., & Richardson, A. D. (2018). Fine-scale perspectives on landscape phenology from unmanned aerial vehicle (UAV) photography. *Agricultural and Forest Meteorology*, *248*, 397–407. https://doi.org/10.1016/j.agrformet.2017.10.015

Knohl, A., Schulze, E.-D., Kolle, O., & Buchmann, N. (2003). Large carbon uptake by an unmanaged 250-year-old deciduous forest in Central Germany. *Agricultural and Forest Meteorology*, *118*(3–4), 151–167. https://doi.org/10.1016/S0168-1923(03)00115-1

Knohl, A., Siebicke, L., Tiedemann, F., Kolle, O., & ICOS Ecosystem Thematic Centre. (2022). *Warm winter 2020 ecosystem eddy covariance flux product from Hainich*. https://doi.org/10.18160/CR66-PJ24

Kowalski, T., & Holdenrieder, O. (2009). Pathogenicity of *Chalara fraxinea*. *Forest Pathology*, *39*(1), 1–7. https://doi.org/10.1111/j.1439-0329.2008.00565.x

Lang, W., Chen, X., Qian, S., Liu, G., & Piao, S. (2019). A new process-based model for predicting autumn phenology: How is leaf senescence controlled by photoperiod and temperature coupling? *Agricultural and Forest Meteorology*, *268*, 124–135. https://doi.org/10.1016/j.agrformet.2019.01.006

Lasslop, G., Reichstein, M., Papale, D., Richardson, A. D., Arneth, A., Barr, A., Stoy, P., & Wohlfahrt, G. (2010). Separation of net ecosystem exchange into assimilation and respiration using a light response

curve approach: Critical issues and global evaluation. *Global Change Biology*, *16*(1), 187–208. https://doi.org/10.1111/j.1365-2486.2009.02041.x

Liu, F., Wang, X., & Wang, C. (2019). Autumn phenology of a temperate deciduous forest: Validation of remote sensing approach with decadal leaf-litterfall measurements. *Agricultural and Forest Meteorology*, *279*, 107758. https://doi.org/10.1016/j.agrformet.2019.107758

Liu, G., Chen, X., Zhang, Q., Lang, W., & Delpierre, N. (2018). Antagonistic effects of growing season and autumn temperatures on the timing of leaf coloration in winter deciduous trees. *Global Change Biology*, *24*(8), 3537–3545. https://doi.org/10.1111/gcb.14095

Liu, Q., Fu, Y. H., Zeng, Z., Huang, M., Li, X., & Piao, S. (2016). Temperature, precipitation, and insolation effects on autumn vegetation phenology in temperate China. *Global Change Biology*, *22*(2), 644–655. https://doi.org/10.1111/gcb.13081

Liu, Q., Fu, Y. H., Zhu, Z., Liu, Y., Liu, Z., Huang, M., Janssens, I. A., & Piao, S. (2016). Delayed autumn phenology in the Northern Hemisphere is related to change in both climate and spring phenology. *Global Change Biology*, *22*(11), 3702–3711. https://doi.org/10.1111/gcb.13311

Lu, X., & Keenan, T. F. (2022). No evidence for a negative effect of growing season photosynthesis on leaf senescence timing. *Global Change Biology*, *28*(9), 3083–3093. https://doi.org/10.1111/gcb.16104

Marchand, L. J., Dox, I., Gričar, J., Prislan, P., Leys, S., van den Bulcke, J., Fonti, P., Lange, H., Matthysen, E., Peñuelas, J., Zuccarini, P., & Campioli, M. (2020). Inter-individual variability in spring phenology of temperate deciduous trees depends on species, tree size and previous year autumn phenology. *Agricultural and Forest Meteorology*, *290*, 108031. https://doi.org/10.1016/j.agrformet.2020.108031

Mariën, B., Balzarolo, M., Dox, I., Leys, S., Lorène, M. J., Geron, C., Portillo-Estrada, M., AbdElgawad, H., Asard, H., & Campioli, M. (2019). Detecting the onset of autumn leaf senescence in deciduous forest trees of the temperate zone. *The New Phytologist*, *224*(1), 166–176. https://doi.org/10.1111/nph.15991

McKinney, L. V., Nielsen, L. R., Hansen, J. K., & Kjær, E. D. (2011). Presence of natural genetic resistance in *Fraxinus excelsior* (Oleraceae) to *Chalara fraxinea* (Ascomycota): An emerging infectious disease. *Heredity*, *106*(5), 788–797. https://doi.org/10.1038/hdy.2010.119

Meier, U. (2018). Growth stages of mono- and dicotyledonous plants: BBCH monograph. Open Agrar Repositorium https://www.openagrar.de/receive/openagrar_mods_00042351, https://doi.org/10.5073/20180906-074619

Melaas, E. K., Sulla-Menashe, D., Gray, J. M., Black, T. A., Morin, T. H., Richardson, A. D., & Friedl, M. A. (2016). Multisite analysis of land surface phenology in North American temperate and boreal deciduous forests from Landsat. *Remote Sensing of Environment*, *186*, 452–464. https://doi.org/10.1016/j.rse.2016.09.014

Menzel, A., & Fabian, P. (1999). Growing season extended in Europe. *Nature*, *397*(6721), 659. https://doi.org/10.1038/17709

Menzel, A., Yuan, Y., Matiu, M., Sparks, T., Scheifinger, H., Gehrig, R., & Estrella, N. (2020). Climate change fingerprints in recent European plant phenology. *Global Change Biology*, *26*, 2599–2612. https://doi.org/10.1111/gcb.15000

Norby, R. J. (2021). Comment on "Increased growing-season productivity drives earlier autumn leaf senescence in temperate trees". *Science*, *371*(6533), eabg1438. https://doi.org/10.1126/science.abg1438

Peñuelas, J., Rutishauser, T., & Filella, I. (2009). Phenology feedbacks on climate change. *Science*, *324*(5929), 887–888. https://doi.org/10.1126/science.1173004

Piao, S., Friedlingstein, P., Ciais, P., Viovy, N., & Demarty, J. (2007). Growing season extension and its impact on terrestrial carbon cycle in the Northern Hemisphere over the past 2 decades. *Global Biogeochemical Cycles*, *21*(3), GB3018. https://doi.org/10.1029/2006GB002888

Piao, S., Liu, Q., Chen, A., Janssens, I. A., Fu, Y., Dai, J., Liu, L., Lian, X., Shen, M., & Zhu, X. (2019). Plant phenology and global climate change: Current progresses and challenges. *Global Change Biology*, *25*(6), 1922–1940. https://doi.org/10.1111/gcb.14619

Queloz, V., Grünig, C. R., Berndt, R., Kowalski, T., Sieber, T. N., & Holdenrieder, O. (2011). Cryptic speciation in *Hymenoscyphus albidus*. *Forest Pathology*, *41*(2), 133–142. https://doi.org/10.1111/j.1439-0329.2010.00645.x

R Core Team. (2022). *R: A language and environment for statistical computing*. https://www.R-project.org/

Reichstein, M., Falge, E., Baldocchi, D., Papale, D., Aubinet, M., Berbigier, P., Bernhofer, C., Buchmann, N., Gilmanov, T., Granier, A., Grünwald, T., Havránková, K., Ilvesniemi, H., Janous, D., Knohl, A., Laurila, T., Lohila, A., Loustau, D., Matteucci, G., … Valentini, R. (2005). On the separation of net ecosystem exchange into assimilation and ecosystem respiration: Review and improved algorithm. *Global Change Biology*, *11*(9), 1424–1439. https://doi.org/10.1111/j.1365-2486.2005.001002.x

Richardson, A. D., Black, T. A., Ciais, P., Delbart, N., Friedl, M. A., Gobron, N., Hollinger, D. Y., Kutsch, W. L., Longdoz, B., Luyssaert, S., Migliavacca, M., Montagnani, L., Munger, J. W., Moors, E., Piao, S., Rebmann, C., Reichstein, M., Saigusa, N., Tomelleri, E., … Varlagin, A. (2010). Influence of spring and autumn phenological transitions on forest ecosystem productivity. *Philosophical Transactions of the Royal Society of London. Series B, Biological Sciences*, *365*(1555), 3227–3246. https://doi.org/10.1098/rstb.2010.0102

Richardson, A. D., Keenan, T. F., Migliavacca, M., Ryu, Y., Sonnentag, O., & Toomey, M. (2013). Climate change, phenology, and phenological control of vegetation feedbacks to the climate system. *Agricultural and Forest Meteorology*, *169*, 156–173. https://doi.org/10.1016/j.agrformet.2012.09.012

Ryu, Y., Lee, G., Jeon, S., Song, Y., & Kimm, H. (2014). Monitoring multilayer canopy spring phenology of temperate deciduous and evergreen forests using low-cost spectral sensors. *Remote Sensing of Environment*, *149*, 227–238. https://doi.org/10.1016/j.rse.2014.04.015

Sagi, O., & Rokach, L. (2018). Ensemble learning: A survey. *WIREs Data Mining and Knowledge Discovery*, *8*(4), e1249. https://doi.org/10.1002/widm.1249

Smith, A. M., & Ramsay, P. M. (2020). A comparison of ground-based methods for obtaining large-scale, high-resolution data on the spring leaf phenology of temperate tree species. *International Journal of Biometeorology*, *64*(3), 521–531. https://doi.org/10.1007/s00484-019-01839-2

Soudani, K., Delpierre, N., Berveiller, D., Hmimina, G., Pontailler, J.-Y., Seureau, L., Vincent, G., & Dufrêne, É. (2021). A survey of proximal methods for monitoring leaf phenology in temperate deciduous forests. *Biogeosciences*, *18*(11), 3391–3408. https://doi.org/10.5194/bg-18-3391-2021

Stéfanon, M., Drobinski, P., D'Andrea, F., & Noblet-Ducoudré, N. d. (2012). Effects of interactive vegetation phenology on the 2003 summer heat waves. *Journal of Geophysical Research Biogeosciences*, *117*(D24). https://doi.org/10.1029/2012JD018187

Stener, L.-G. (2013). Clonal differences in susceptibility to the dieback of *Fraxinus excelsior* in southern Sweden. *Scandinavian Journal of Forest Research*, *28*(3), 205–216. https://doi.org/10.1080/02827581.2012.735699

Tamrakar, R., Rayment, M. B., Moyano, F., Mund, M., & Knohl, A. (2018). Implications of structural diversity for seasonal and annual carbon dioxide fluxes in two temperate deciduous forests. *Agricultural and Forest Meteorology*, *263*, 465–476. https://doi.org/10.1016/j.agrformet.2018.08.027

Templ, B., Koch, E., Bolmgren, K., Ungersböck, M., Paul, A., Scheifinger, H., Rutishauser, T., Busto, M., Chmielewski, F.-M., Hájková, L., Hodzić, S., Kaspar, F., Pietragalla, B., Romero-Fresneda, R., Tolvanen, A., Vučetič, V., Zimmermann, K., & Zust, A. (2018). Pan

European phenological database (PEP725): A single point of access for European data. *International Journal of Biometeorology*, *62*(6), 1109–1113. https://doi.org/10.1007/s00484-018-1512-8

Thiel, C., Mueller, M. M., Epple, L., Thau, C., Hese, S., Voltersen, M., & Henkel, A. (2020). UAS imagery-based mapping of coarse wood debris in a natural deciduous forest in Central Germany (Hainich National Park). *Remote Sensing*, *12*(20), 3293. https://doi.org/10.3390/rs12203293

Uphus, L., Lüpke, M., Yuan, Y., Benjamin, C., Englmeier, J., Fricke, U., Ganuza, C., Schwindl, M., Uhler, J., & Menzel, A. (2021). Climate effects on vertical Forest phenology of *Fagus sylvatica* L., sensed by Sentinel-2, time lapse camera, and visual ground observations. *Remote Sensing*, *13*(19), 3982. https://doi.org/10.3390/rs13193982

Wilhite, D. A., & Glantz, M. H. (1985). Understanding: The drought phenomenon: The role of definitions. *Water International*, *10*(3), 111–120. https://doi.org/10.1080/02508068508686328

Wu, C., Chen, J. M., Black, T. A., Price, D. T., Kurz, W. A., Desai, A. R., Gonsamo, A., Jassal, R. S., Gough, C. M., Bohrer, G., Dragoni, D., Herbst, M., Gielen, B., Berninger, F., Vesala, T., Mammarella, I., Pilegaard, K., & Blanken, P. D. (2013). Interannual variability of net ecosystem productivity in forests is explained by carbon flux phenology in autumn. *Global Ecology and Biogeography*, *22*(8), 994–1006. https://doi.org/10.1111/geb.12044

Wu, C., Gough, C. M., Chen, J. M., & Gonsamo, A. (2013). Evidence of autumn phenology control on annual net ecosystem productivity in two temperate deciduous forests. *Ecological Engineering*, *60*, 88–95. https://doi.org/10.1016/j.ecoleng.2013.07.019

Wutzler, T., Lucas-Moffat, A., Migliavacca, M., Knauer, J., Sickel, K., Šigut, L., Menzer, O., & Reichstein, M. (2018). Basic and extensible post-processing of eddy covariance flux data with REddyProc. *Biogeosciences*, *15*(16), 5015–5030. https://doi.org/10.5194/bg-15-5015-2018

Xie, Y., Wang, X., & Silander, J. A. (2015). Deciduous forest responses to temperature, precipitation, and drought imply complex climate change impacts. *Proceedings of the National Academy of Sciences of the United States of America*, *112*(44), 13585–13590. https://doi.org/10.1073/pnas.1509991112

Xie, Y., Wang, X., Wilson, A. M., & Silander, J. A. (2018). Predicting autumn phenology: How deciduous tree species respond to weather stressors. *Agricultural and Forest Meteorology*, *250-251*, 127–137. https://doi.org/10.1016/j.agrformet.2017.12.259

Yuan, Y., Härer, S., Ottenheym, T., Misra, G., Lüpke, A., Estrella, N., & Menzel, A. (2021). Maps, trends, and temperature sensitivities-phenological information from and for decreasing numbers of volunteer observers. *International Journal of Biometeorology*, *65*(8), 1377–1390. https://doi.org/10.1007/s00484-021-02110-3

Zani, D., Crowther, T. W., Mo, L., Renner, S. S., & Zohner, C. M. (2020). Increased growing-season productivity drives earlier autumn leaf senescence in temperate trees. *Science*, *370*(6520), 1066–1071. https://doi.org/10.1126/science.abd8911

Zeng, L., Wardlow, B. D., Xiang, D., Hu, S., & Li, D. (2020). A review of vegetation phenological metrics extraction using time-series, multispectral satellite data. *Remote Sensing of Environment*, *237*, 111511. https://doi.org/10.1016/j.rse.2019.111511

Zhao, B., Donnelly, A., & Schwartz, M. D. (2020). Evaluating autumn phenology derived from field observations, satellite data, and carbon flux measurements in a northern mixed forest, USA. *International Journal of Biometeorology*, *64*(5), 713–727. https://doi.org/10.1007/s00484-020-01861-9

Zhou, S., Zhang, Y., Caylor, K. K., Luo, Y., Xiao, X., Ciais, P., Huang, Y., & Wang, G. (2016). Explaining inter-annual variability of gross primary productivity from plant phenology and physiology. *Agricultural and Forest Meteorology*, *226-227*, 246–256. https://doi.org/10.1016/j.agrformet.2016.06.010

Zhou, S., Zhang, Y., Ciais, P., Xiao, X., Luo, Y., Caylor, K. K., Huang, Y., & Wang, G. (2017). Dominant role of plant physiology in trend and variability of gross primary productivity in North America. *Scientific Reports*, *7*, 41366. https://doi.org/10.1038/srep41366

Zohner, C. M., Mirzagholi, L., Renner, S. S., Mo, L., Rebindaine, D., Bucher, R., Palouš, D., Vitasse, Y., Fu, Y. H., Stocker, B. D., & Crowther, T. W. (2023). Effect of climate warming on the timing of autumn leaf senescence reverses after the summer solstice. *Science*, *381*(6653), eadf5098. https://doi.org/10.1126/science.adf5098

Zohner, C. M., & Renner, S. S. (2019). Ongoing seasonally uneven climate warming leads to earlier autumn growth cessation in deciduous trees. *Oecologia*, *189*(2), 549–561. https://doi.org/10.1007/s00442-019-04339-7

SUPPORTING INFORMATION

Additional supporting information can be found online in the Supporting Information section at the end of this article.

How to cite this article: Kloos, S., Klosterhalfen, A., Knohl, A., & Menzel, A. (2024). Decoding autumn phenology: Unraveling the link between observation methods and detected environmental cues. *Global Change Biology*, *30*, e17231. https://doi.org/10.1111/gcb.17231